The EMBO Journal Vol.16 No.18 pp.5531–5536, 1997

Neutron crystallographic evidence of lipase–colipase complex activation by a micelle

Juan Hermoso[1], David Pignol, Simon Penel[2], Michel Roth, Catherine Chapus[3] and Juan Carlos Fontecilla-Camps[4]

Laboratoire de Cristallographie et de Cristallogenèse des Protéines, Institut de Biologie Structurale Jean-Pierre Ebel, CEA-CNRS, 41 Avenue des Martyrs, 38027 Grenoble Cedex 1, [2]Large Scale Structures Group, Institut Laue-Langevin, BP 156, 38042 Grenoble and [3]Laboratoire de Bioénergétique et d'Ingénierie des Protéines, UPR 9036 CNRS, BP 71, 13402 Marseille Cedex 9, France

[1]Present address: Departamento de Cristallografia, Instituto 'Rocasolano', CSIC, Serrano 119, 28006 Madrid, Spain

[4]Corresponding author

J.Hermoso and D.Pignol contributed equally to this work

The concept of lipase interfacial activation stems from the finding that the catalytic activity of most lipases depends on the aggregation state of their substrates. It is thought that activation involves the unmasking and structuring of the enzyme's active site through conformational changes requiring the presence of oil-in-water droplets. Here, we present the neutron structure of the activated lipase–colipase–micelle complex as determined using the D_2O/H_2O contrast variation low resolution diffraction method. In the ternary complex, the disk-shaped micelle interacts extensively with the concave face of colipase and the distal tip of the C-terminal domain of lipase. Since the micelle- and substrate-binding sites concern different regions of the protein complex, we conclude that lipase activation is not interfacial but occurs in the aqueous phase and is mediated by colipase and a micelle.

Keywords: hydrolase/interfacial activation/lipid/neutron diffraction

Introduction

Lipases (triacylglyceride esther hydrolase, EC 3.1.1.3) hydrolyse triglycerides at a lipid–water interface. They differ from classic esterases in that their activity is dramatically increased upon binding to the lipid surface (Sarda and Desnuelle, 1958). In vertebrates, where triacylglycerol hydrolysis is carried out largely by pancreatic lipases (PL), the accumulation of amphiphiles at the oil–water interface should prevent PL binding. In the duodenum, where the oil-in-water droplets are covered by several natural surfactants, the problem is circumvented by the presence of colipase (CL), a pancreatic polypeptide that helps productive PL binding to the emulsified oil droplets (Hofman and Small, 1967). Our understanding of PL activation and catalysis has improved dramatically in the last few years thanks to the elucidation of the three-dimensional structure of the uncomplexed human enzyme by Winkler *et al.* (1990) and of a human PL–porcine CL complex obtained in the presence of mixed micelles by van Tilbeurgh *et al.* (1993). In the human enzyme, a large amphiphilic loop (the flap) covers the active site channel, offering an explanation for the limited catalytic activity of PL in solution. The PL–CL structure (van Tilbeurgh *et al.*, 1993), in turn, shows that the active site is exposed and the flap makes a series of polar contacts with CL. Together, these structures have provided a comprehensive view of the changes likely to take place during activation: as in the analogous case of fungal enzymes (Brzozowski *et al.*, 1991), the flap uncovers the active site that undergoes a conformational change, adopting the catalytically active configuration. In addition, the process generates a hydrophobic surface ~50 Å long (van Tilbeurgh *et al.*, 1993), providing a plausible structural basis for the interaction of the PL–CL complex with tri- (TG) and diglyceride (DG) substrates.

We have very recently reported the X-ray structure of the porcine PL–CL complex from crystals obtained in the presence of the non-ionic detergent tetraethylene glycol monooctyl ether (C_8E_4) (Hermoso *et al.*, 1996). In that structure, PL was found to be in the open conformation (Figure 1), a result we attributed to the presence of detergent micelles in the crystallization medium. In agreement with these conclusions, we have also shown that solution inhibition of PL by the serine-specific inhibitor diisopropyl *p*-nitrophenylphosphate (E600), a reaction that requires an exposed active site, can only occur in the presence of PL, CL and supermicellar concentrations of either non-ionic detergents or bile salts (Hermoso *et al.*, 1996).

Neutron diffraction coupled to D_2O/H_2O contrast variation [a technique commonly used in small angle scattering experiments (Timmins and Zaccai, 1988)] is the only available method for studying disordered detergent in crystals. It has been used previously to determine the structure of detergent bound to photoreaction centers (Roth *et al.*, 1989), to locate bound lipid in the lipovitellin complex (Timmins *et al.*, 1992), to study the distribution of RNA and protein in the interior of tomato bushy stunt virus (Timmins *et al.*, 1994a) and to define the detergent structure in porin crystals (Pebay-Peyroula *et al.*, 1995). Here, we report the results of a series of experiments using low resolution neutron diffraction at the DB21 station of the Institut Laue-Langevin (ILL, Grenoble, France) carried out to establish the possible presence of detergent micelles in our PL–CL complex crystals.

Results and discussion

A lipase–colipase–micelle ternary complex

Figure 2 shows the X-ray PL–CL model (Hermoso *et al.*, 1996) along with a part of the resulting neutron solvent-

flattened low resolution negative scattering-length map calculated at the protein match point (Table I). The most remarkable feature of this 'detergent' map is the large distorted disk-shaped density that contacts the concave face of CL and the lower tip of the C-terminal domain of PL. Since our study was aimed primarily at locating the bound micelle, no attempts were made to distinguish the polar head groups from the hydrophobic core by using pre-deuterated detergent (Pebay-Peyroula *et al.*, 1995). The overall shape and size of the observed micelle (an ellipsoid with semi-axes of 23 Å×13 Å×11 Å) correspond to those expected for C_8E_4 (Timmins *et al.*, 1994b) if, as proposed by Tanford (1972), the observed minor semi-axis corresponds to the length of the C_8E_4 tail. Assuming a perfect elliptical shape, the micelle calculated volume is 13 770 $Å^3$. However, this value is likely to be an underestimate since the polar heads may display low constrast under the experimental conditions. Using the reported volumes for both complete C_8E_4 (504 $Å^3$) and the protonated C_8 fragment (237 $Å^3$) (Zulauf and Rosenbusch, 1983), limit values of 27 and 58 detergent molecules per micelle are found, respectively. These values are in good agreement with the aggregation number of 68 molecules per micelle determined for the closely related detergent C_8E_5 (Timmins *et al.*, 1994b).

The micelle sits in a roughly spherical cavity and binds two PL–CL complexes which are related by a

Fig. 1. Schematic representation of the porcine PL–CL complex. The PL molecule is depicted in blue, except for the flap region which is shown in gold. CL is shown in purple. Binding of CL to PL helps stabilize the open configuration of the flap, exposing the active site and generating an extensive hydrophobic surface. This surface is formed by several loops of CL, parts of the flap and regions around the active site of PL (see also Figure 5).

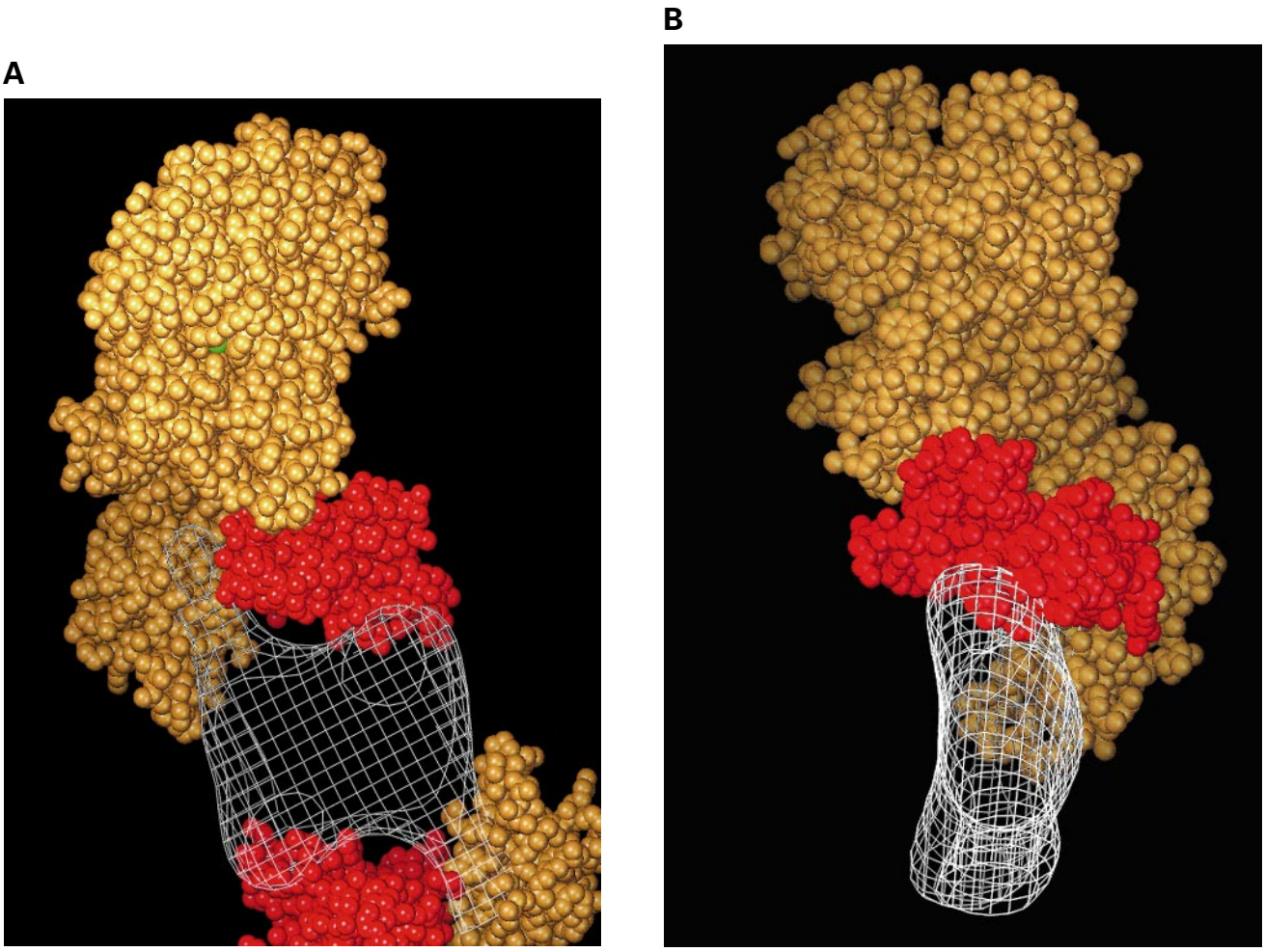

Fig. 2. The PL–CL–micelle complex. The neutron negative scattering-length solvent-flattened map was calculated at the protein match point (41% D_2O) and contoured at the 1 σ level. PL (gold) and CL (red) are depicted as CPK models. (**A**) Depiction of the map corresponding to the C_8E_4 micelle bound to two PL–CL complexes related by a crystallographic 2-fold axis. (**B**) The same PL–CL–micelle complex rotated by 90° about the vertical axis (the lower truncated PL–CL complex has been omitted for clarity).

Table I. Data collection and refinement statistics

Data sets (18 Å resolution)				
D_2O content (%)	No. of observations	Unique reflections	Completeness (%)	R_{sym}
0	563	96	88.0	0.06
22.5	202	79	72.5	0.11
59.7	816	104	95.4	0.07
83.5	692	103	94.5	0.05

Refinement		
Model	Initial *R*-factor	Final *R*-factor
Protein (11% D_2O)	0.31	0.31 (0.23)
Detergent (41% D_2O)	0.59	0.38 (0.29)
Solvent	0.43	0.31 (0.29)

Initial *R*-factors were calculated as $(\Sigma_h F_{int} - F_{calc})/\Sigma_h F_{int}$, where F_{int} are interpolated to either protein or detergent match points from the observed *F*s. F_{calc} were calculated by nYn. Final *R*-factors were calculated similarly except that F_{calc} were obtained after density modification using DM (Collaborative Computational Project Number 4, 1994). Final *R*-factor values in parenthesis were calculated using a 1 σ cut-off (56 reflections left).

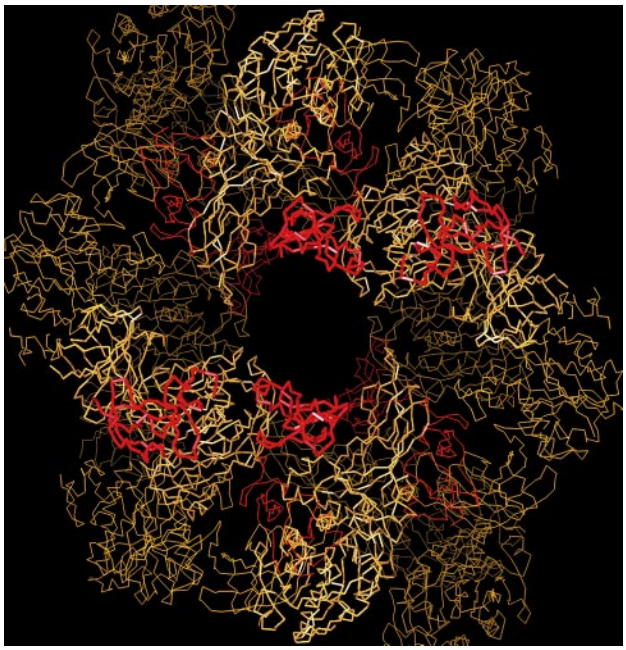

Fig. 3. Crystal packing of the porcine PL–CL complex (Hermoso *et al.*, 1996). The upper central PL–CL complex is depicted in the same orientation as in Figures 1 and 2A. The packing generates cylindrical channels, perpendicular to the plane of the paper, occupied by a series of detergent micelles intercalated with solvent pockets. PL (gold) and CL (red) are depicted as Cα backbones. The large central cavity lodges a C_8E_4 micelle (see Figure 2).

crystallographic 2-fold axis (Figure 3). The CL–micelle contacts are mostly mediated by residues in the 70–85 loop although many other residues are involved (see Figure 4). PL–micelle contacts are restricted mainly to segments comprising residues 367–373, 384–387, 401–404 and 408–412. Thus there is no direct interaction between the micelle and the active site region of PL. In contrast with what is generally observed with membrane proteins (Michel, 1991), the protein surfaces involved in micelle binding are amphipathic without forming patches

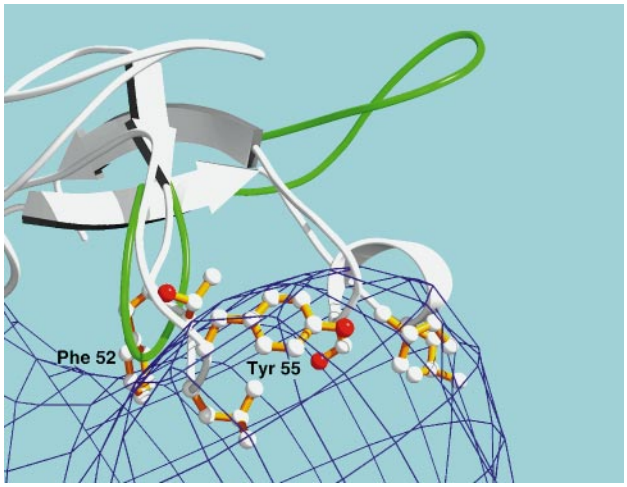

Fig. 4. Binding of CL to the detergent micelle. The bound CL (white) is compared with the average NMR solution structure of the cofactor. For the latter, only loops with significantly different orientations are depicted (green) (Breg *et al.*, 1995). Reorganization of CL upon binding to the micelle involves an 82° rotation, the generation of an α-helix in the 70–85 loop and conformational changes of loop 49–58. Several residues seem to bind the detergent micelle. The highlighted Phe52 (W52 in horse CL) and Tyr55 residues have been found to bind TDC micelles in solution (Canioni *et al.*, 1981; McIntyre *et al.*, 1987). The map is the one already described in Figure 2.

of either hydrophilic or hydrophobic amino acid side chains. The micelle interacts more extensively with CL than with PL, in agreement with the fact that uncomplexed CL binds taurodeoxycholate (TDC) micelles (Sari *et al.*, 1978; Charles *et al.*, 1980; Cozzone *et al.*, 1981; Larsson and Erlanson-Albertsson, 1981; McIntyre *et al.*, 1987) whereas PL does not (Morgan *et al.*, 1969). The longest axis of the micelle and that of CL are roughly perpendicular (Figure 2B), as in the model of Charles *et al.* (1980) who used low angle neutron scattering to determine the size and shape of a CL–TDC micelle complex. When compared with its average NMR solution structure (Breg *et al.*, 1995), the crystalline CL displays an 82° rotation of the loop comprising residues 70–85, a movement that is most likely due to the interaction of several of its hydrophobic side chains with the micelle (Figure 4). Many residues from other regions of CL, both polar and hydrophobic, are also found at the CL–micelle interface (Figure 4). Corroborating indirect evidence for micelle binding by the cofactor has been obtained for two of these residues: a dansyl derivative of Tyr55 of porcine CL (McIntyre *et al.*, 1987) and Trp52 of the equine cofactor (which corresponds to a Phe residue in the porcine CL) (Canioni *et al.*, 1981; McIntyre *et al.*, 1987). Neither of these residues is part of the hydrophobic surface described by van Tilbeurgh *et al.* (1993).

Micelle size-dependent affinity

The presence of a C_8E_4 micelle in the porcine PL–CL complex has prompted us to examine the crystal packing of the open human–porcine complex obtained in the presence of supermicellar concentrations of bile salts, phospholipids and octyl-β-glucopyranoside (van Tilbeurgh *et al.*, 1993). As in our case, CL and the lower half of the C-terminal domain of PL face a cavity that could contain a micelle of similar dimensions to those found in

Table II. E600 inhibition of pancreatic lipase in the presence of bile salt micelles

Lipase (10^{-6} M)	Colipase (10^{-5} M)	Bile salt (mM)	E600 (mM)	$t_{50\%}$ (min)
6.0	1.2	4.0	2.5	8 ± 1
6.0	1.2	16.0[a]	2.5	80 ± 10
0.1	0.2	4.0	0.5	40 ± 5
0.01	0.02	4.0	0.5	50 ± 10

The experiments were carried out as reported (Hermoso *et al.*, 1996) at pH 6.0 and 20°C in the presence of 0.1 M NaCl. $t_{50\%}$ is the time needed to reach 50% lipase inhibition. The bile salt used was sodium taurodeoxycholate (TDC) except ([a]) = sodium taurocholate (TC). No inhibition was observed in the absence of either colipase or bile salt (not shown). TC, that forms much smaller aggregates than TDC (4–7 and 22–24 monomers per aggregate, respectively; Hofman and Small, 1967), displays significantly slower inhibition kinetics. This effect on PL activation may reflect size-dependent changes in micelle binding affinity to the enzyme and the cofactor.

our crystals (not shown). This similarity suggests that the concavity of the complex binding site may restrict the size of the binding micelle to a rather narrow range (Figure 1). The neutron scattering study by Charles *et al.* (1980) has shown that the bound TDC micelle can be described as a prolate with a radius close to 10 Å and axial ratio of ~2. These dimensions are similar to those of our C_8E_4 micelle. Also, the center-to-center distance in the colipase–TDC micelle complex is given as 29 Å, a value that is similar to the one observed by us (27–30 Å) in the crystal structure. These observations strongly suggest that the size and mode of interaction of TDC micelles are very similar to those of C_8E_4 in the crystallographic ternary complex. TC and TDC, although very closely related, form aggregates of significantly different sizes (aggregation numbers of 4–7 and 22–24, respectively; Hofman and Small, 1967). We have taken advantage of this fact to study the influence of this parameter on PL inhibition by E600 (Table II). In the presence of TC, the inhibition kinetics are significantly slower, showing that the smaller TC micelle does not activate the enzyme efficiently.

In vivo conditions

The vast body of *in vitro* results concerning PL activation need to be explained in terms of the *in vivo* conditions. Ultracentrifuged duodenal contents extracted from human subjects after ingestion of a fat-rich meal have been shown to contain, on the one hand, oil-in-water emulsion particles with cores of TG, DG and cholesterol esters, emulsified with a surface coat of fatty acids, monoglycerides, phospholipids and bile salts, and, on the other, saturated mixed micelles of bile salts, fatty acids, 'acid soaps', monoglycerides, phospholipids, cholesterol and traces of TG and DG along with unilamellar vesicles (Hernell *et al.*, 1990). Two general mechanisms of physiological adsorption of PL and CL to the oil-in-water emulsion particles have been proposed: (i) binding of CL to the emulsified substrate, followed by PL–CL complex formation (anchoring) (Chapus *et al.*, 1975; Patton *et al.*, 1978) and (ii) formation of a PL–CL–lipid (or lipoprotein) complex prior to substrate binding (Lairon *et al.*, 1978; Bernbäck *et al.*, 1989; Hernell *et al.*, 1990). Which mechanism is likely to be physiologically relevant can be determined by the relative binding affinity of CL for PL, mixed micelles and emulsified oil drops. In the presence of mixed fatty acids–bile salt micelles and absence of substrate, CL dissociates from PL with a K_d of ~10^{-8} M (Larsson and Erlanson-Albertsson, 1981) making the CL–PL association stronger than either CL or PL binding to emulsified substrate. Physiologically, a significant fraction of enzyme and cofactor will be complexed in the micelle-rich aqueous phase since, under these conditions, the CL–PL K_d is ~10 times lower than their respective duodenal concentrations (Borgstrom and Hildebrand, 1975). Our own E600 inhibition experiments in solution indicate that even homogeneous TDCNa micelles can open the PL flap in the presence of CL at physiologically relevant concentrations (Table II). Taken together, these results favor a mechanism where PL adsorption to the emulsified oil droplets is mediated by a pre-formed ternary PL–CL–mixed micelle complex.

Lipase activation occurs in the aqueous phase

In contrast to fungal lipases, where binding to hydrophobic oil droplets to elicit activation seems to be possible (Brzozowski *et al.*, 1991), PL is exposed to a predominantly hydrophilic environment: the water phase in the intestinal lumen, mixed micelles and emulsified oil drops. As shown by *in vitro* experiments, this environment is unlikely to provide a direct driving force for activation because it should favor the closed configuration of PL. We believe that, by binding to CL and PL, the mixed micelle indirectly helps to stabilize the PL open flap configuration. Thus in the duodenal PL–CL–micelle complex, an otherwise unfavorable conformation of PL is generated, exposing extensive hydrophobic regions to the aqueous environment. Burying such hydrophobic regions into the lipid phase of the substrate droplet should be energetically favorable and thus facilitate catalysis (Figure 6). CL plays a central role in the ternary complex by being able to bind to three different partners: the PL C-terminal domain and the flap, a mixed micelle, and an oil-in-water particle. The geometry of the observed ternary complex (Figures 2 and 5) does not require the displacement of the bound micelle upon binding to the interface surface since the micelle does not cover the extensive PL–CL hydrophobic surface described by van Tilbeurgh *et al.* (1993) (Figure 6). The ultimate fate of the bound micelle is unknown. It may (i) dissociate from the PL–CL complex upon binding to the interface; (ii) while bound, accumulate product and subsequently leave the interface, momentarily disrupting the ternary complex which will be re-formed by addition of a new, product-poor micelle, or (iii) remain bound to LP and CL throughout catalysis.

When compared with the fungal enzymes, pancreatic lipases display a more complex activation process, a direct consequence of the coating of duodenal oil drops by natural surfactants. Besides the already well-documented role played by CL in opening the PL flap, we have shown here that mixed micelles are also very likely to be essential to this process. In the duodenum, the binding of mixed micelles to the PL–CL complex may provide a fine-tuned control of lipolysis and help the evacuation of products from the oil drops as mixed fatty acid–monoglyceride–bile salt micelles that subsequently are absorbed by intestinal enterocytes (Shiau, 1987). This is, to our knowledge, the

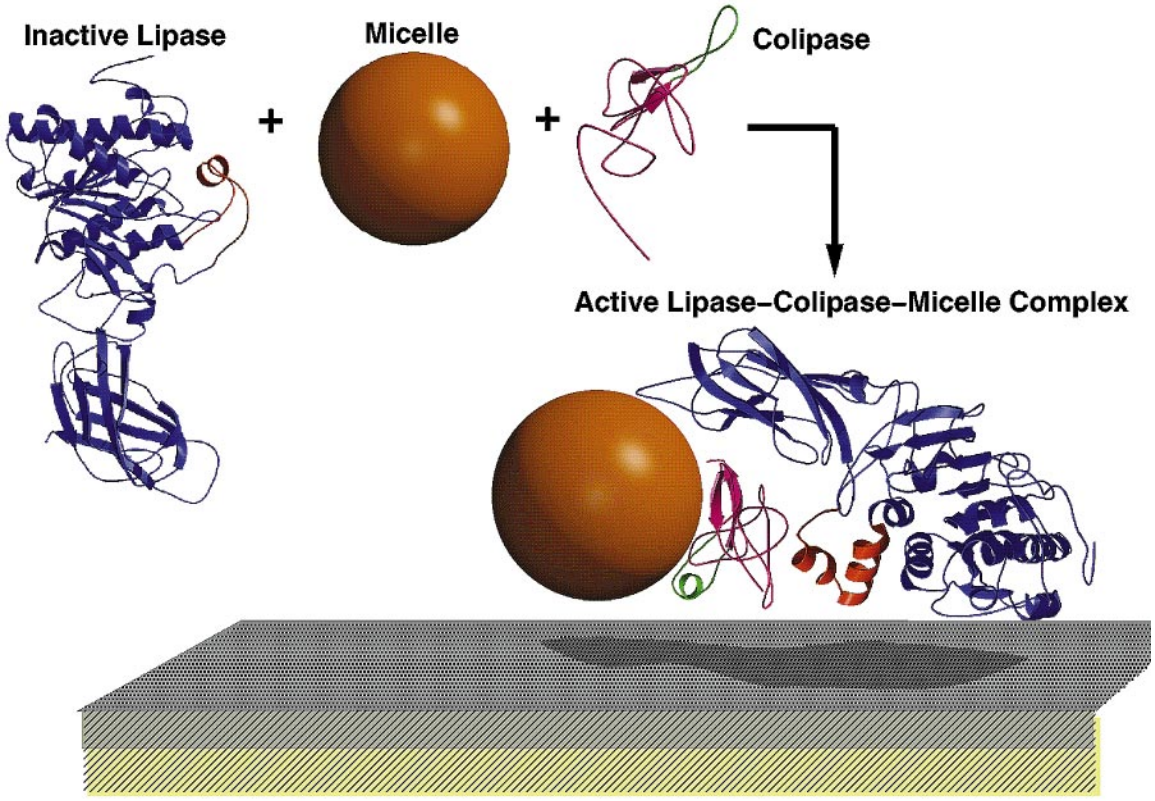

Fig. 5. Schematic depiction of PL activation in solution by CL and a duodenal mixed micelle. The formation of a complex between inactive PL (van Tilbeurgh *et al.*, 1992), CL and a mixed micelle activates the enzyme by stabilizing the flap in the open conformation and exposing a large hydrophobic surface. This surface should facilitate complex binding to the underlying tri- and diglycerides of the emulsified duodenal oil particle. The particle polar layer and underlying substrates (not drawn to scale) are depicted in gray and yellow respectively. The uncomplexed CL is shown as the procolipase NMR solution (Breg *et al.*, 1995).

first time a micelle is visualized as part of an enzymatic complex without displaying extensive hydrophobic interaction with the protein moieties, as in membrane proteins. From these results, we conclude that micelle and substrate binding by PL–CL concern different regions of the protein complex and that the activation of PL is not an interfacial phenomenon.

Materials and methods

Crystallization

Porcine PL and CL were both purified from a delipidated acetonic pancreatic powder as previously described (Hermoso *et al.*, 1996). Crystals for neutron diffraction were grown from solutions containing 0.6 M ammonium sulfate, MES 0.1 M pH 6 and 15 mM C_8E_4 (Hermoso *et al.*, 1996). It should be noted that crystallization attempts using detergent concentrations below its critical micelle concentration (CMC; 7 mM) were systematically unsuccessful. Crystals were transferred into the mother liquor at room temperature, and soaked for 3 weeks on several changes of the same saline solution containing the appropriate D_2O/H_2O ratio. The D_2O content of the crystals was checked by neutron transmission measurements of the mother liquor from which the crystals were taken. Crystals of maximum dimension 0.4 mm^3 were mounted in quartz capillaries.

Data collection

Data from single crystals soaked in mother liquor containing 0, 22.5, 59.7 and 83.5% D_2O were measured on the four-circle diffractometer at the DB21 beam line, ILL, Grenoble. The neutron wavelength was 7.536 Å and the crystal–detector distance 250 mm. Data were collected at 0.15° intervals with a 30 min exposition time per image. The orientation matrix and the preliminary refinement of the cell parameters and camera constants were carried out using MAINDEX (Penel and Legrand, 1997). The PL–CL complex crystallizes in the cubic F23 space group (a = 290 Å) but it displays a strong P23 pseudosymmetry (Hermoso *et al.*, 1996). Because of the low resolution of the analysis, all procedures were carried out in the space group P23 (a = 145 Å).

Data reduction

Data were reduced using a suite of programs written by M.Roth, A.Lewit-Bentley and G.Bentley (unpublished). Analytically predicted reflection masks (Roth and Lewit-Bentley, 1982) were used for integration of reflection intensities from the area detector two-dimensional images. Statistics on the number of unique reflections per contrast, completeness and consistency of the data are summarized in Table I.

Scaling and phasing

The scaling and phasing of the data were carried out using the new program nYn written by one of us (M.R.). nYn first scales the contrast variation data measured on different crystals. Subsequently, given the phased protein structure factors (Fs), it calculates the best Fs of the density maps defining the solvent and detergent envelopes (Roth, 1991). The phases of the solvent and detergent density maps were improved independently with the density modification program DM (Collaborative Computational Project Number 4, 1994). The new solvent and detergent Fs calculated by DM, together with the protein Fs, were input to nYn for a new best F calculation, the whole process being iterated a few times. The protein Fs are the ones calculated using the X-ray atomic coordinates of the molecule at the contrast where the scattering-length densities of detergent and solvent are nearly equal (11% D_2O). The detergent Fs calculated by nYn are those corresponding to protein, detergent and solvent at the contrast where the scattering-length densities of protein and solvent are nearly equal (41% D_2O).

Scattering-length map calculations

Scattering-length maps were calculated using the FTT program (Collaborative Computational Project Number 4, 1994).

Figures were prepared using O (Jones *et al.*, 1991), Molscript (Kraulis, 1991) and Render 3D (Merritt and Murphy, 1994).

Acknowledgements

We thank Dr Brigitte Kerfelec and Dr Isabelle Crenon for fruitful discussions and encouragement. We also thank Dr Eva Pebay-Peroula for help at the DB21 neutron beam line of the ILL and Dr Peter Timmins for neutron transmission measurements. This work is dedicated to the memory of Professor P.Desnuelle.

References

Bernbäck,S., Bläckberg,L. and Hernell,O. (1989) Fatty acids generated by gastric lipase promote human milk triacylglycerol digestion by pancreatic colipase-dependent-lipase. *Biochim. Biophys. Acta*, **1001**, 286–293.

Borgstrom,B. and Hildebrand,H. (1975) Lipase and colipase activity on human small intestinal contents after a liquid fat meal. *Scand. J. Gastroenterol.*, **10**, 585–591

Breg,J.N., Sarda,L., Cozzone,P.J., Rugani,N., Boelens,R. and Kaptein,R. (1995) Solution structure of porcine pancreatic procolipase as determined from ^{1}H homonuclear two-dimensional and three dimensional NMR. *Eur J. Biochem.*, **227**, 663–672.

Brzozowski,A.M. *et al*. (1991) A model for interfacial activation in lipases from the structure of a fungal lipase–inhibitor complex. *Nature*, **351**, 491–494.

Canioni,P., Julien,R., Romanetti,R., Cozzone,P. and Sarda,L. (1981) Circular dichroism study of horse colipase interaction with bile salt. *Biochim. Biophys. Acta*, **670**, 305–311.

Chapus,C., Sari,H., Semeriva,M. and Desnuelle,P. (1975) Role of colipase in the interfacial adsorption of pancreatic lipase at a hydrophilic interface. *FEBS Lett.*, **58**, 155–158.

Charles,M., Semeriva,M. and Chabre,M. (1980) Small-angle neutron scattering study of the association between porcine pancreatic colipase and taurodeoxycholate micelles. *J. Mol. Biol.*, **139**, 297–317.

Collaborative Computational Project Number 4 (1994) The CCP4 suite: programs for protein crystallography. *Acta Crystallogr.*, **D50**, 760–763.

Cozzone,P., Canioni,P., Sarda,L. and Kaptein,R. (1981) 360-MHz nuclear magnetic resonance and laser photochemically induced dynamic nuclear polarization studies of bile salt interactions with porcine colipase A. *Eur. J. Biochem.*, **114**, 119–126.

Hermoso,J., Pignol,D., Kerfelec,B., Crenon,I., Chapus,C. and Fontecilla-Camps,J.C. (1996) Lipase activation by nonionic detergents, the crystal structure of the porcine lipase–colipase–tetraethylene glycol monooctyl ether complex. *J. Biol. Chem.*, **271**, 18007–18016.

Hernell,O., Staggers,J.E. and Carey,M.C. (1990) Physical-chemical behavior of dietary and biliary lipids during intestinal digestion and absorption. Phase analysis and aggregation states of luminal lipids during duodenal fat digestion in healthy adult human beings. *Biochemistry*, **29**, 2041–2056.

Hofmann,A. and Small,D.M. (1967) Detergent properties of bile salts: correlation with physiological function. *Annu. Rev. Med.*, **18**, 333–376.

Jones,T.A., Zou,J.Y., Cowan,S.W. and Kjeldgaard,M. (1991) Improved methods for building protein models in electron density maps and the location of errors in these models. *Acta Crystallogr.*, **D47**, 110–119.

Kraulis,P.J. (1991) MOLSCRIPT: a program to produce both detailed and schematic plots of proteins. *J. Appl. Crystallogr.*, **24**, 946–950.

Lairon,D., Nalbone,G., Lafont,H., Leonardi,J., Domingo,N., Hauton,J.C. and Verger,R. (1978) Possible roles of bile lipids and colipase in lipase adsorption. *Biochemistry*, **17**, 5263–5269.

Larsson,A. and Erlanson-Albertsson,C. (1981) The identity and properties of two forms of activated colipase from porcine pancreas. *Biochim. Biophys. Acta*, **664**, 538–548.

McIntyre,J.C., Hundley,P. and Behnke,D. (1987) The role of aromatic side chain residues in micelle binding by pancreatic colipase. *Biochem. J.*, 245, 821–829.

Merritt,E.A. and Murphy,M.E.P. (1994) Raster3D version 2.0 a program for photorealistic molecular graphics. *Acta Crystallogr.*, **D50**, 869–873.

Michel,H. (1991) General and practical aspects of membrane protein crystallization. In Michel,H. (ed.), *Crystallization of Membrane Proteins*. CRC Press, Boca Raton, FL, pp. 63–88.

Morgan,R.G.H., Barrowma,J. and Börgstrom,B. (1969) The effect of sodium taurodeoxycholate and pH on the gel filtration behaviour of rat pancreatic protein and lipases. *Biochim. Biophys. Acta*, **175**, 65–75.

Patton,J.S., Albertsson,P.A., Erlanson,C. and Börgstrom,B. (1978) Binding of porcine pancreatic lipase and colipase in the absence of substrate studied by two-phase partition and affinity chromatography. *J. Biol. Chem.*, **253**, 4195–4202.

Penel,S. and Legrand,P. (1997) MAINDEX—manual indexation for area-detector crystallographic data. *J. Appl. Crystallogr.*, **30**, 206.

Pebay-Peyroula,E., Garavito,R.M., Rosenbusch,J.P., Zulauf,M. and Timmins,P.A. (1995) Detergent structure in tetragonal crystals of Ompf porin. *Structure*, **3**, 1051–1059.

Roth,M. (1991) Phasing at low resolution. In Moras,D., Podjarny,A. and Thierry,J.C. (eds), *Crystallographic Computing 5. International Union of Crystallography.* Oxford University Press, Oxford, UK, pp. 229–248.

Roth,M and Lewit-Bentley,A. (1982) Low-resolution diffractometry with a position-sensitive multidetector. *Acta Crystallogr.*, **A38**, 670–679.

Roth,M., Lewit-Bentley,A., Michel,H., Deisenhofer,J., Huber,R. and Oesterhelt,D. (1989) Detergent structure in crystals of a bacterial photosynthetic reaction centre. *Nature*, **340**, 659–662.

Sarda,L and Desnuelle,P. (1958) Action de la lipase pancreatique sur les esters en emulsion. *Biochim. Biophys. Acta*, **30**, 513–521.

Sari,H., Granon,S. and Semeriva,M. (1978) Role of tyrosine residues in the binding of colipase to taurodeoxycholate micelles. *FEBS Lett.*, **95**, 229–234.

Shiau,Y.F. (1987) Lipid digestion and absorption. In Johnson,L.R. (ed.), *Physiology and Gastrointestinal Tract*. Raven Press, New York, pp. 1527–1534.

Tanford,C. (1972) Micelle shape and size. *J. Phys. Chem.*, 76, 3020–3024.

Timmins,P.A. and Zaccai,J. (1988) Low resolution structures of biological complexes studied by neutron scattering. *Eur. Biophys. J.*, **15**, 157–168.

Timmins,P.A., Poliks,B. and Banaszak,L. (1992) The location of bound lipid in the lipovitellin complex. *Science*, **257**, 652–655.

Timmins,P.A., Wild,D. and Witz,J. (1994a) The three-dimensional distribution of RNA and protein in the interior of tomato bushy stunt virus: a neutron low-resolution single-crystal diffraction study. *Structure*, **2**, 1191–1201.

Timmins,P.A., Pebay-Peyroula,E. and Welte,W. (1994b) Detergent organisation in solutions and in crystals of membrane proteins. *Biophys. Chem.*, **53**, 27–36.

van Tilbeurgh,H., Sarda,L., Verger,R. and Cambillau,C. (1992) Structure of the pancreatic lipase–procolipase complex. *Nature*, **359**, 159–162.

van Tilbeurgh,H., Egloff,M.P., Martinez,C., Rugani,N., Verger,R. and Cambillau,C. (1993) Interfacial activation of the lipase–procolipase complex by mixed micelles revealed by X-ray crystallography. *Nature*, **362**, 814–820.

Winkler,F.K., D'Arcy,A. and Hunziker,W. (1990) Structure of human pancreatic lipase. *Nature*, **343**, 771–774.

Zulauf,M. and Rosenbush,J.P. (1983) Micelle clusters of octylhydroxyoligo(oxyethylenes). *J. Phys. Chem.*, **87**, 855–862.

Received on April 7, 1997; revised on May 21, 1997